Direct Determination of Photodisintegration Cross Sections and the p-process

H. Utsunomiya [a] P. Mohr [b] A. Zilges [c] M. Rayet [d]

[a] *Department of Physics, Konan University, 8-9-1 Okamoto, Higashinada, Kobe 658-8501, Japan*

[b] *Strahlentherapie, Diakoniekrankenhaus Schwäbisch Hall, D–74523 Schwäbisch Hall, Germany*

[c] *Institut für Kernphysik, Technische Universität Darmstadt, Schlossgartenstraße 9, D-64289 Darmstadt, Germany*

[d] *Institut d'Astronomie et d'Astrophysique, Université Libre de Bruxelles, Campus de la Plaine, CP226, 1050 Brussels, Belgium.*

Abstract

Photon-induced reactions play a key role in the nucleosynthesis of heavy neutron-deficient nuclei, the so-called p-nuclei. In this paper we review the present status of experiments on photon-induced reactions at energies of astrophysical importance and their relevance to p-process modeling.

Key words: Nucleosynthesis; photon-induced reactions; p-process

1 Introduction

The p-nuclei refer to stable, heavy nuclides that are neutron-deficient and can not, for that reason, be produced in stars by the slow or rapid neutron capture chains (s- or r-processes), unlike the majority of heavy nuclei with charge number in excess of the value $Z = 26$ (Fe). Thirty-five nuclei are classically considered as p-nuclei, with Z ranging from 34 (Se) to 80 (Hg), although 5 of them can also be produced to some extend by the s-process. All p-nuclei can be synthesized from the destruction of pre-existing seed nuclei of the s- and r-type by a combination of (p,γ) captures and (γ,n), (γ,p) or (γ,α) photoreactions. Complemented by some β^+, electron captures and (n,γ) reactions, those nuclear flows are referred to as the p-process. That p-nuclei are produced from existing s- or r-seed nuclei is comforted by the fact that in

the solar system they represent only a small fraction (0.01 to 1%, exceptionally of the order of 10%), of the isotopic content of the corresponding elements.

The (p,γ) reactions require both high temperatures and large proton densities and appear to contribute only and probably marginally, to the production of the lightest p-nuclei. Photodisintegrations are thus expected to play the leading role in the p-process. Temperatures in excess of about $T_9 = 1.5$ ($T_9 = T/10^9$ K, where T is the temperature in Kelvin) are required for photodisintegrations to take place on time scales comparable to stellar evolutionary ones, and may not exceed $T_9 = 3.5$ in order to avoid the photoerosion of all the heavy nuclei to the more stable nuclei of the "iron peak". It is also necessary to freeze-out the photodesintegrations on a short enough time-scale, typically of the order of one second. Those constraints are nicely satisfied in the deep O-Ne-rich layers of massive stars exploding as type II supernovae (SNe-II). The SN-II is undoubtedly the most studied and the most satisfactory scenario for the p-process (1; 2; 3). Other plausible sites for the p-process, like pre-supernova burning phases of massive stars or the explosion of type Ia supernovae, have also been explored (see (4) for a very complete review of those works).

In order to estimate the number of photoreactions per unit of time in a given volume of a star at temperature T, one has to integrate over the energy E the cross section $\sigma(E)$ weighted by the photon energy distribution $n_\gamma(E,T)$ times the speed of light c. As Sect.2 will show more quantitatively, only the high energy tail of $n_\gamma(E,T)$ contributes to the rate, the integrand being non-negligible only on a relatively narrow window of photon energies. Knowing $n_\gamma(E,T)$, one might expect photodisintegration rates to be determined easily by the measurement of the cross section on that energy range, typically a few MeV in the 1–10 MeV domain (Sect. 2).

However, direct determinations of reaction rates for the p-process suffer from two major limitations. The first is the fact that the p-process involves thousands of photoreactions (not to speak of the secondary nuclear transmutations mentioned above) and that most of the involved nuclei are unstable, which means that only a tiny fraction of those reactions can be measured in the laboratory. The second limitation is that in a gas at high temperature, excited levels of the target nuclei are populated according to the Boltzmann statistics, so that photoreactions on excited levels must be taken into account. This thermalization effect is specially important here because of the high temperatures involved in the p-process and because photodisintegrations are specially sensitive to threshold effects. This is illustrated in Sect. 3 in the case of (γ,n) reactions.

If the direct determination of astrophysical rates at work in the p-process is clearly out of reach, experimental studies of photodisintegration cross sections in the relevant energy range and for nuclei as close as possible to the neu-

tron deficient side of the valley of stability are of crucial importance to test the nuclear reaction models used to calculate the rates. Valuable pieces of information are also obtained, more traditionally, by the measurement of cross sections in the reverse, radiative capture channel. They can indeed be used to constrain the calculation of the rates in the photoreaction channel via the reciprocity theorem. One must keep in mind however that such measurements are but a fragment of the information needed for the calculation of the reverse rate. To be correct, such a calculation requires the knowledge of all non negligible cross sections from any excited state of the target nucleus to any state of the residual one.

Direct measurements of photodisintegration cross sections constitute therefore an independent set of data and the most straightforward way to constrain the calculation of the corresponding astrophysical rate. Real-photon source facilities have been developed and the interest of some of these facilities for the study of the p-process is discussed in the present paper [1] . After generalities on photon-induced reactions in Sect. 2, Sect. 3 presents some results for (γ,n) reactions obtained at the bremsstrahlung facility of the Technische Universität Darmstadt. It is a nice feature of bremsstrahlung facilities that they can be tuned to produce photon spectra which approximate the high energy part of the Planck spectrum for temperatures of interest for the p-process. The obtained experimental rate can be directly compared to the calculated rate for photoreaction on a ground-state nucleus.

Quasi-monochromatic photon beams with tunable energy can be obtained using the technique of laser inverse-Compton scattering. This technique has been successfully applied recently to nuclear astrophysics at the National Institute of Advanced Industrial Science and Technology in Japan and is described in Sect. 4. The excitation function provided by such experiments is extremely useful information to check theoretical models of nuclear reactions. Section 5 presents some results of (γ, γ') experiments, providing direct insight into the γ-strength below the particle threshold. All the experiments described in this paper shed new light on the low-energy tail of the γ-ray strength in nuclei and are therefore expected to improve the rate predictions.

Improving the theoretical predictions for photodisintegration rates will put p-process nucleosynthesis calculations on a firmer ground. As mentioned before the p-process takes place at very high temperatures but the nuclei involved are in a region of the nuclear chart where basic quantities like masses or β-decay rates are either known or rather reliably estimated. Experimental data on photoreaction cross sections, even scarce, are therefore a very precious ingredient to test the validity of Hauser-Feshbach cross section calculations in

[1] In this paper, we exclude virtual-photon sources like electron scattering and Coulomb excitation.

the nuclear region of interest. Sect. 6 briefly discusses the impact of such data on the production of the p-nuclei, in relation with the uncertainties inherent to the envisioned astrophysical scenarios. Sect. 6 also discusses a few examples where the production of a p-nuclide is directly related to the measurement of specific photonuclear cross sections.

Finally, perspectives for new experimental techniques and measurements related to astrophysical problems are presented in Sect. 7 with emphasis on an insertion light source of the SPring-8, a synchrotron radiation facility of the third generation. Conclusions are drawn in Sect. 8.

2 Basic considerations on photon-induced reactions

2.1 Photoreactions on nuclei in the ground state

The reaction rate $\lambda_{(\gamma,j)}$ for a photoreaction induced on a ground-state nucleus, leading to the emission of particle j is given by the expression :

$$\lambda_{(\gamma,j)} = \int_0^\infty c\, n_\gamma(E)\, \sigma_{(\gamma,j)}(E)\, dE \tag{1}$$

where c is the speed of light, $\sigma_{(\gamma,j)}$ the cross section and $n_\gamma(E)$ the number of photons per unit volume and energy E. In a stellar interior at a temperature T, $n_\gamma(E)$ is remarkably close to a black-body or Planck distribution:

$$n_\gamma(E,T)\, dE = \frac{1}{\pi^2}\, \frac{1}{(\hbar c)^3}\, \frac{E^2}{\exp\left(E/kT\right) - 1}\, dE \qquad . \tag{2}$$

It has its maximum at energies around $E \approx \frac{3}{2}kT$ which is of the order of a few hundred keV in the temperature range $1.5 \leq T_9 \leq 3.5$ ($T_9 = 1$ corresponds to $kT = 86\,\mathrm{keV}$). At energies of several MeV the photon density is governed by the exponential decrease in Eq. 2.

If Eq. 2 is substituted for $n_\gamma(E)$ in Eq. 1, the rate becomes a function of the parameter T. It is then possible to define the photon energy range which is the most relevant for determining $\lambda_{(\gamma,j)}(T)$ at the temperatures of astrophysical interest. This results from the properties of the integrand of Eq. 1 which differs significantly from zero only in a relatively small energy range. We call this range the Gamow window by reference to the case of reactions induced by charged particles in a thermalized environment, where the entrance channel

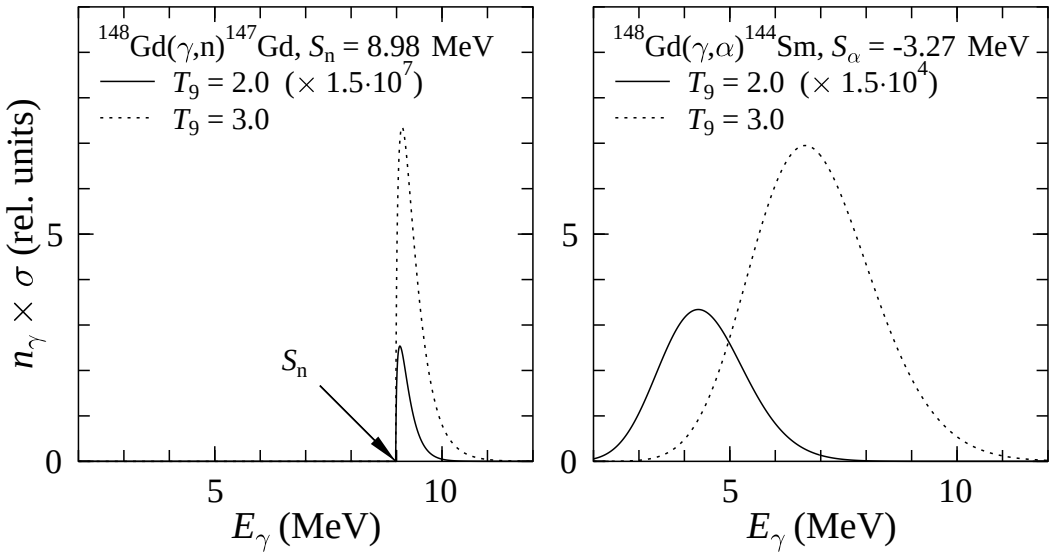

Fig. 1. Gamow window (integrand of Eq. 1) for (γ,n) (left panel) and (γ,α) reactions (right panel) on the ground state of the target nucleus ^{148}Gd, with separation energies $S_n = 8.98\,\mathrm{MeV}$ and $S_\alpha = -3.27\,\mathrm{MeV}$. Note the temperature dependence of the position of the Gamow window when the emitted particle is charged as well as the significant changes of the vertical scales in both panels when T_9 goes from 2 to 3.

energy distribution is given by the Maxwell-Boltzmann statistics. Here however one has to distinguish between (γ,n) reactions, where the position of the Gamow window is determined by the reaction threshold, and (γ,p) or (γ,α) reactions where it is shifted and broadened by the Coulomb barrier in the outgoing channel (5).

The (γ,n) cross section close above the threshold S_n can be expressed (6) as

$$\sigma_{(\gamma,\mathrm{n})}(E) = \sigma_0 \times \left(\frac{E - S_\mathrm{n}}{S_\mathrm{n}}\right)^{\ell+1/2} \tag{3}$$

where ℓ is the angular momentum of the emitted neutron. Eqs. 2 and 3 locate the maximum of the integrand in Eq. 1 at $E = S_\mathrm{n} + kT/2$ for $\ell = 0$ (7; 8; 9). The corresponding narrow Gamow window is shown in Fig. 1 (left panel) for the temperatures $T_9 = 2.0$ and 3.0. The Gamow window for (γ,n) reactions thus remains close to the reaction threshold for all relevant temperatures. Because of the strong temperature dependence of the photon density, the reaction rate depends sensitively on the temperature; it increases by a factor $6.7 \cdot 10^7$ from $T_9 = 2.0$ to 3.0 for the example shown in Fig. 1.

For the photon-induced emission of charged particles we make the assumption that the astrophysical S-factor is roughly constant for the inverse capture reaction. This leads to a Gamow window for (γ,α) and (γ,p) reactions which peaks at the sum of the separation energy $S_{\alpha,\mathrm{p}}$ and the Gamow window peak

energy E_0 of the inverse capture reaction,

$$E_\gamma = S_{\alpha,\mathrm{p}} + E_0 \quad , \tag{4}$$

and has the same width as the Gamow window of the capture reaction. In contrast to the (γ,n) reaction, the position of the Gamow window for (γ,α) and (γ,p) reactions changes significantly with temperature (see right panel of Fig. 1). However, the temperature dependence of the reaction rate is less strong than in the (γ,n) case. From $T_9 = 2$ to 3 it changes by a factor of $4.4{\cdot}10^4$, i.e. three orders of magnitude less than in the neutron case. Consequently, the branching ratio between (γ,n) and (γ,α) reactions will depend sensitively on the temperature. This remark, which applies also to some extend to the (γ,p) reactions, is of particular importance for the path followed by the nuclear flow in the p-process (see e.g. (10)).

We remark also that in the nuclear mass region of interest for the p-process and not too far from stability, (γ,α) reactions usually have much larger reaction rates than (γ,p) reactions because in that region α particles have small or even negative binding energies, whereas typical proton separation energies are of the order of several MeV. Therefore, when the α particle is replaced by a proton, the smaller Coulomb barrier, reducing E_0 in Eq. 4 by a factor $2^{4/3}$, does not compensate the strong increase in binding energy ($S_p - S_\alpha$) and the (γ,α) reaction operates at significantly lower photon energies, and thus higher photon densities, than the (γ,p) reaction.

Very few experimental data on photodisintegration cross sections are available in the literature at the energies of interest for the p-process. For (γ,n) reactions most of the data have been measured around the giant dipole resonance (GDR) with high precision; however, close to the threshold, the data have typically much larger uncertainties (11). The situation is even worse for (γ,α) reactions, for which the rare available measurements have all been made at energies much higher than the Gamow window (see e.g. (12)). Another difficulty comes from the fact that the p-nuclei are very little abundant naturally and that experiments on those nuclei usually require targets made of a considerable amount of highly enriched material.

2.2 Thermalization effect under stellar conditions

In stellar environments nuclear excited states are thermally populated. At the high temperatures we consider, thermalization may enhance the photoreaction rates by several orders of magnitudes (examples are found in Sect. 3). The right hand side of Eq. 1, which corresponds to photodisintegration from the ground state only, must then be replaced by a sum of the rates $\lambda^{\mu}_{(\gamma,j)}(T)$ for

photodisintegration from all (ground and excited) states μ, each term being weighted by the appropriate Boltzmann factor. The true astrophysical rate λ^* is therefore defined by

$$\lambda^*_{(\gamma,j)}(T) = \frac{1}{G(T)} \sum_{\mu} \frac{(2J^\mu + 1)}{(2J^0 + 1)} \lambda^\mu_{(\gamma,j)}(T) \ \exp\left(-\varepsilon^\mu / kT\right) \quad , \tag{5}$$

where, in $\lambda^\mu_{(\gamma,j)}(T)$, $\sigma_{(\gamma,j)}(E)$ is replaced by the cross section $\sigma^\mu_{(\gamma,j)}(E)$ for photodisintegration from state μ and where $G(T) = \sum_\mu (2J^\mu + 1)/(2J^0 + 1) \exp(-\varepsilon^\mu/kT)$ is the temperature-dependent normalized partition function of the target nucleus.

Although the gross effect of thermalization is a shift of the Gamow window to lower photon energies by some mean excitation energy, it is mandatory to perform the sum explicitly (or, if necessary, to integrate on a model level density for the target), when more than one excited level is populated, which is most often the case for relatively massive nuclei away from shell closures in the considered temperature range.

Clearly the multitude of astrophysical rates needed to describe the nucleosynthesis of the p-nuclei has to be calculated theoretically. In all existing p-process calculations, reaction rates are calculated in the framework of the Hauser-Feshbach (HF) statistical model. We refer to (13; 4; 14) for a description of the HF model and of its underlying hypothesis. Let us just recall here that the HF cross section for the reaction $I^\mu + j \rightarrow L^\nu + k$ where particle j is captured on nucleus I in excited state μ, leaving residual nucleus L in state ν and particle or photon k, is obtained from the transmission coefficients for the formation of or decay from all states J^π of the compound nucleus which can be formed from the quantum numbers of the entrance channel. Since in stellar conditions the target nucleus is in thermal equilibrium it can be shown (13) that the astrophysical rates for the forward and reverse channels of the reaction $I + j \rightarrow L + k$ are symmetrical and therefore obey reciprocity, which is not the case when the target nucleus is in its ground state only. This remains true when k is a photon, so that the photodisintegration rate of a nucleus L leading to particle j and residual nucleus I is directly proportional to the radiative capture rate of particle j on I, $N_A\langle\sigma v\rangle^*_{(j,\gamma)}$, where * means as before that the rate takes target thermalization into account.

We want to emphasize here that as long as the conditions for the application of a statistical model for the reaction cross sections are met, which is the case to a large extend for typical p-process nuclear flows as discussed in Sect. 6, the uncertainties involved in any HF cross section calculation are essentially related to the evaluation of the nuclear quantities necessary for the calculation of the partition functions $G(T)$ as well as the transmission coefficients entering the calculation of $\langle\sigma v\rangle^*_{(j,\gamma)}$. Not only the ground state properties (masses,

deformations, matter densities) of the target and residual nuclei have to be known, or, when not available experimentally, have to be obtained from nuclear mass models, but the excited state properties are also indispensable. Experimental data may be scarce, especially for nuclei located far from the valley of nuclear stability and frequent resort to a level density prescription is mandatory. The transmission coefficients for particle emission are calculated by solving the Schrödinger equation with the appropriate optical potential for the particle-nucleus interaction. The case of the α-nucleus potential is of particular significance for the p-process but suffers from the scarcity of α-nucleus cross section measurements at sub-Coulomb energies, especially for $A > 100$ nuclei, and from the difficulties to construct theoretically global and reliable α-nucleus potentials (see recent attempts in (15; 16) and (4) for a review of the present situation).

In order to obtain reliable predictions for the astrophysical rates, a strict methodology is compulsory: calculated nuclear properties, constrained by indispensable but sporadic experiments, should rely on coherent sets of data, based whenever possible on microscopic models of the nucleus. Extensive work along this line has been performed in the framework of the on-line library BRUSLIB (17) [2].

The photon transmission function requires a particular attention in the case of photonuclear reactions and is calculated assuming the dominance of dipole E1 transitions. Reaction theory relates the γ-transmission coefficient for excited states to the ground state assuming the GDR is built on each excited state and has a Lorentzian representation, at least for medium- and heavy-mass nuclei. Experimental photoabsorption data confirm the simple semi-classical prediction of a Lorentzian shape at energies around the resonance energy, but this description is less satisfactory at lower energies, and especially near the reaction threshold. Even if a direct knowledge of the astrophysical rate of Eq. 5 is not accessible to experiments, photoreaction cross section measurements in the Gamow window energy range will be extremely useful to improve our knowledge of the dipole strength functions at low energy.

3 Photodisintegration measurements with bremsstrahlung

Bremsstrahlung facilities provide intense photon radiation with energies up to the energy of the incoming electron beam. As shown in Sect. 2, the astrophysically relevant energy range is located at several MeV. Hence facilities with electron energies around 10 MeV are best suited for experiments of astrophysical interest.

[2] accessible at url http://www.astro.ulb.ac.be

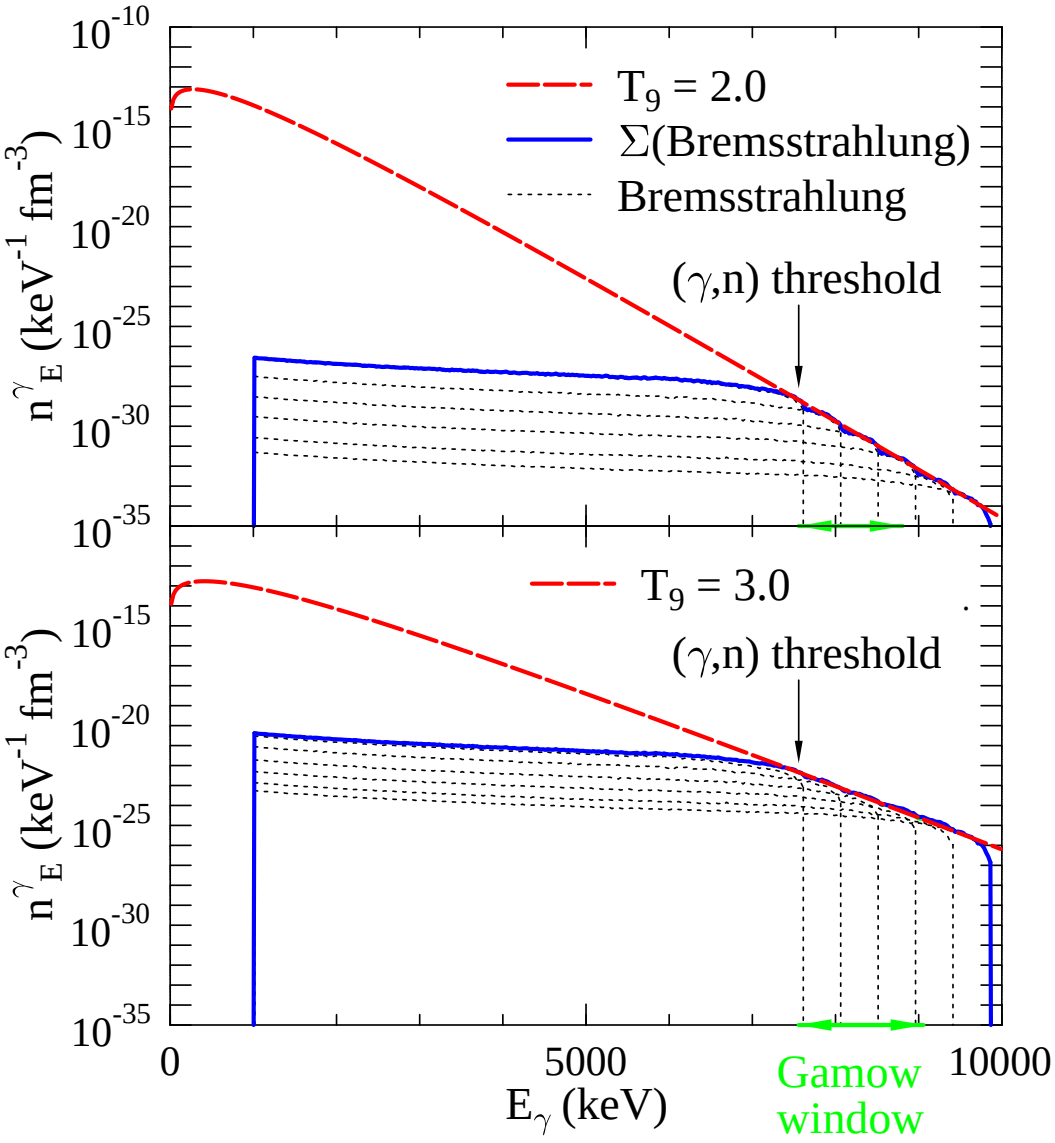

Fig. 2. Approximation of the thermal photon energy distribution (dashed line) by a weighted sum of the end-point portions of bremsstrahlung spectra (full line) for $T_9 = 2$ (upper panel) and $T_9 = 3$ (lower panel), in the corresponding Gamow window, located close above the (γ,n) threshold. The individual bremsstrahlung spectra are shown with dotted lines.

The photoactivation technique, obviously limited to reactions where an unstable nucleus is produced, has been chosen for the experiments using bremsstrahlung because a direct detection of the emitted particle is difficult in the huge bremsstrahlung background. Additionally, the excellent energy resolution of γ-ray detectors allows a clear detection of the individual reaction even in a chemically mixed target with natural isotopic composition. For example, a clear photoactivation signal has been observed for the ^{190}Pt(γ,n)^{189}Pt reaction with a ^{190}Pt mass of about 100 μg (i.e. 0.014 % natural abundance of ^{190}Pt in a 800 mg natural platinum target). The disadvantage of a low overall

Table 1
Experimental results for (γ,n) reaction rates, $\lambda_{\rm exp}^{\rm g.s.}$, for $T_9 = 2.5$ (experimental uncertainties are given in parentheses). They are compared to theoretical predictions for photodisintegration from the target ground state: $\lambda_{\rm th}^{\rm g.s.}$(M) and $\lambda_{\rm th}^{\rm g.s.}$(MST) are calculated with the code MOST (see text) and $\lambda_{\rm th}^{\rm g.s.}$(NS) is the prediction of the code Non-Smoker. Additionally the rate λ^* for a thermalized target and the corresponding enhancement factor $\lambda^*/\lambda_{\rm th}^{\rm g.s.}$(NS) are also shown. All rates are in $\rm s^{-1}$.

nucleus	$\lambda_{\rm exp}^{\rm g.s.}$	$\lambda_{\rm th}^{\rm g.s.}$(M)	$\lambda_{\rm th}^{\rm g.s.}$(MST)	$\lambda_{\rm th}^{\rm g.s.}$(NS)	λ^*	$\lambda^*/\lambda_{\rm th}^{\rm g.s.}$(NS)
^{186}W	$3.1(4)\cdot10^{2}$	$1.1–2.8\cdot10^{2}$	$2.5\cdot10^{2}$	$2.6\cdot10^{2}$	$1.0\cdot10^{5}$	$4.0\cdot10^{2}$
^{185}Re	$1.9(7)\cdot10^{1}$	$1.0–4.7\cdot10^{1}$	$4.4\cdot10^{1}$	$1.9\cdot10^{1}$	$2.5\cdot10^{4}$	$1.3\cdot10^{3}$
^{187}Re	$7.6(7)\cdot10^{1}$	$1.9–8.2\cdot10^{1}$	$7.0\cdot10^{1}$	$7.2\cdot10^{1}$	$8.4\cdot10^{4}$	$1.2\cdot10^{3}$
^{190}Pt	$4(2)\cdot10^{-1}$	$1.1–4.8\cdot10^{-1}$	$2.9\cdot10^{-1}$	$1.8\cdot10^{-1}$	$1.0\cdot10^{3}$	$5.5\cdot10^{3}$
^{192}Pt	$5(2)\cdot10^{-1}$	$0.2–1.3\cdot10^{0}$	$5.6\cdot10^{-1}$	$5.8\cdot10^{-1}$	$1.9\cdot10^{3}$	$3.3\cdot10^{3}$
^{198}Pt	$8.7(2)\cdot10^{1}$	$0.34–1.3\cdot10^{2}$	$1.1\cdot10^{2}$	$5.0\cdot10^{1}$	$1.5\cdot10^{4}$	$3.1\cdot10^{2}$
^{197}Au	$6.2(8)\cdot10^{0}$	$2.7–9.1\cdot10^{0}$	$5.6\cdot10^{0}$	$4.8\cdot10^{0}$	$5.1\cdot10^{3}$	$1.1\cdot10^{3}$
^{196}Hg	$4.2(7)\cdot10^{-1}$	$2.0–7.5\cdot10^{-1}$	$5.8\cdot10^{-1}$	$3.2\cdot10^{-1}$	$5.4\cdot10^{2}$	$1.7\cdot10^{3}$
^{198}Hg	$2.0(3)\cdot10^{0}$	$0.77–3.0\cdot10^{0}$	$2.1\cdot10^{0}$	$1.4\cdot10^{0}$	$1.0\cdot10^{3}$	$7.5\cdot10^{2}$
^{204}Hg	$5.7(9)\cdot10^{1}$	$0.47–1.9\cdot10^{2}$	$1.7\cdot10^{2}$	$7.3\cdot10^{1}$	$3.1\cdot10^{3}$	$4.3\cdot10^{1}$
^{204}Pb	$1.9(3)\cdot10^{0}$	$0.98–3.8\cdot10^{0}$	$3.0\cdot10^{0}$	$1.5\cdot10^{0}$	$2.5\cdot10^{2}$	$1.6\cdot10^{2}$

detection efficiency, which is of the order of a few per cent in the best cases, is compensated by the huge number of photons in the bremsstrahlung beam. This results in typical measuring times of a few days.

The general set-up of photoactivation experiments is simple. Here we describe the set-up used at the TU Darmstadt (18). Electrons with energies up to 10 MeV and currents up to about 50 μA are provided by the superconducting linear accelerator S-DALINAC. The electron beam is completely stopped in a massive copper radiator. The bremsstrahlung is collimated and hits the target roughly 1.5 m behind the radiator. For normalization, the incoming photons are monitored by photon scattering in the ^{11}B(γ,γ')^{11}B* reaction (see Sect. 5). Typical photon intensities are of the order of $10^4 - 10^5$ $\rm keV^{-1}\,cm^{-2}\,s^{-1}$. Alternatively a relative measurement can be carried out using a standard with well-known cross section and suitable properties for photoactivation (low photoneutron threshold, reasonable half-life, strong γ-ray lines after β-decay, high natural abundance). The ^{197}Au(γ,n)^{196}Au reaction has already been used successfully (19), and measurements have been performed to establish ^{187}Re as another standard (20). Excellent agreement has been found between experiments using bremsstrahlung/photoactivation and monochromatic photons/direct neutron detection, for both standard nuclei ^{197}Au and ^{187}Re. A relative measurement can also be made putting the target very close

to the radiator, where the photon intensity is roughly a factor of 300 higher than at the position behind the collimator. After photoactivation the γ-rays from the decay of the produced nuclei are measured using a high-purity germanium detector.

The analysis of bremsstrahlung data is complicated because of the broad energy spectrum of the bremsstrahlung photons. The experimental yield Y is proportional to

$$Y \sim \int_{S_n}^{E_0} \sigma(E)\, N_\gamma(E, E_0)\, dE \quad , \tag{6}$$

where $N_\gamma(E, E_0)$ is the number of photons per keV and cm^2 in the bremsstrahlung spectrum with endpoint energy E_0. Unfolding procedures have been used to extract the cross section $\sigma(E)$, but such procedures are limited by significant systematic errors. Alternatively, a reasonable assumption on the threshold behavior or a theoretical prediction for $\sigma(E)$ can be used to solve the integral in Eq. 6; in this case the experimental result is just a normalization factor for the theoretical prediction.

Recently, a new method has been established to derive the ground state reaction rates λ by approximating the black-body photon density $n_\gamma(E, T)$ (Eq. 2) by a weighted sum of bremsstrahlung spectra with different endpoint energies $E_{0,i}$:

$$c\, n_\gamma(E, T) \approx \sum_i a_i(T)\, N_\gamma(E, E_{0,i}) \quad , \tag{7}$$

where $a_i(T)$ is a set of weighting coefficients for a given value of T. The excellent agreement between the thermal distribution and the weighted sum in the relevant energy window close above the threshold is shown in Fig. 2 for $T_9 = 2.0$ and $T_9 = 3.0$; hence the weighted sum of bremsstrahlung spectra may be called a "quasi–thermal" spectrum with variable temperature. Up to now results have been obtained for a number of nuclei which are listed in Tab. 1 [3] . The values $\lambda_{\rm exp}^{\rm g.s.}$ are derived from bremsstrahlung experiments with a superposition of spectra (Eq. 7) corresponding to a temperature $T_9 = 2.5$. Those values are compared to theoretical predictions for photodisintegration from the target ground state. Column $\lambda_{\rm th}^{\rm g.s.}$(M) shows the minimum and maximum values of the rates calculated with the code MOST (21), for 14 different sets of the nuclear data necessary to calculate the HF cross sections, and $\lambda_{\rm th}^{\rm g.s.}$(MST)

[3] Minor differences between the values in Tab. 1 and already published numbers come from an improved analysis of the shape of the bremsstrahlung spectra close to the endpoint energy.

are MOST "standard" values (see (4) and (22) for Re). The rates $\lambda_{\rm th}^{\rm g.s.}$(NS) were derived (23) from cross sections calculated with the code Non-Smoker (such cross sections can be found in (24)). The importance of the target thermalization is well illustrated in the last two columns which show the rates λ^* for a thermalized target as well as the corresponding enhancement factors (23). It is clear that the thermalization effect depends strongly on the detailed level structure of the target nucleus and cannot be estimated by purely qualitative arguments.

Table 1 shows that there is never a strong disagreement between experimental data and theoretical predictions and that no systematic trend for over- or under-estimate of the experimental data can be traced from the present data on very heavy nuclei. The experimental data lie within the ranges of values spanned by the MOST rates obtained with different but reasonable choices of nuclear physics data. The ratio of the maximum to the minimum values never exceeds 6.5, which is a rather favorable situation (4). However, the extreme values do not necessarily correspond to the same set of nuclear physics data so that the comparison made in Table 1 can not be used to discriminate between the different nuclear physics ingredients used in the HF calculations.

4 Photodisintegration measurements with laser inverse-Compton scattering γ rays

The inverse Compton scattering was first studied theoretically in collisions of cosmic rays on thermal photons in space (25). The idea of producing γ rays in the laboratory by interactions between laser photons and relativistic electrons was born in 1963 (26; 27). Technical facets of the idea for practical use were developed in the 1980's (28) but the application of this technique to astronuclear physics had been ignored until recently.

Head-on collisions of laser photons with relativistic electrons produce γ rays with an energy given to an excellent approximation by,

$$E_\gamma = \frac{4\gamma^2 \varepsilon_L}{1 + (\gamma\theta)^2 + 4\gamma\varepsilon_L/(mc^2)}, \tag{8}$$

where $\gamma = E_e/mc^2$, E_e is the electron beam energy and m its rest mass, ε_L is the laser photon energy, and θ the scattering angle of laser photons with respect to the electron beam. Either a conventional laser or a free-electron laser (29) can be employed. The angle $\theta = 0$ corresponds to the maximum of E_γ, as well as of the cross section for photon scattering, according to the Klein-Nishina formula. Also at that angle the polarization of the laser photon is conserved. Collimating scattered photons at $\theta \sim 0$ produces γ rays with

energy spread, $\Delta E_\gamma/E_\gamma = [(2\Delta E_e/E_e)^2 + (\gamma\Delta\theta)^4]^{1/2}$(30). In practice, this energy spread is determined by $\Delta\theta = (\theta_e^2+\theta_c^2)^{1/2}$, where θ_e is the electron beam divergence and θ_c the collimator half angle, rather than by the energy spread of the electron beam $\Delta E_e/E_e$. By changing either the electron beam energy or the laser wavelength, the laser inverse-Compton scattering plays the role of a *photon accelerator*, producing a γ-ray beam that is energy-variable, quasi–monochromatic and linearly- (or circularly-)100% polarized. That technique is superior to the positron annihilation in flight because the latter is beset with the positron bremsstrahlung (11).

4.1 Measurements with the LCS γ beam at AIST

Fine pencil-like beams (typically 2 mm in diameter) of γ rays are available based upon the laser inverse-Compton scattering (LCS) at the National Institute of Advanced Industrial Science and Technology (AIST) (31). Their production utilizes the conventional lasers (Nd:YLF and Nd:YVO) in both Q-switch and CW modes and electron beams in the storage ring TERAS. The γ energy is varied in the region of 1 - 40 MeV by tuning the electron beam energy from 200 to 800 MeV. An energy resolution of 1 - 10 % in FWHM and nearly 100% polarization are achieved. Because of the monochromaticity, the LCS γ beam is best suited to excitation function measurements of photoneutron reactions near threshold with enriched-target material of the order of 1g. In addition, photo-activation of natural foils can be done for nuclei whose isotopic abundance is sufficiently large.

The AIST-LCS γ-beam with a rather limited intensity (10^{4-5} photons/sec) has been used to measure cross sections of ^{9}Be(γ,n)$\alpha\alpha$ of interest for the nucleosynthesis in supernovae (32; 33), of ^{181}Ta(γ,n)^{180}Ta for the p-process nucleosynthesis (34), and D(γ,n)p for big bang nucleosynthesis (35). More recently, photoneutron cross sections have been measured on the ^{186}W, ^{187}Re, and ^{188}Os nuclei, of interest for s-process nucleosynthesis and cosmochronometry, as well as on ^{93}Nb and ^{139}La for p-process studies. In these studies, a 4π-type detection of neutrons was carried out; the latest version of the neutron detector consists of double rings with a total 16 ^{3}He proportional counters embedded in a polyethylene moderator with an overall detection efficiency up to 46% depending on neutron energy. The average energy of neutrons emitted in photodisintegration of medium/heavy nuclei at a given E_γ was determined by the so-called ring ratio, the ratio of neutrons detected by the inner and outer rings of 8 ^{3}He counters each. Typical time for measuring the excitation function over the Gamow window is 1 hour per energy, thanks to large GDR cross sections even in the tail region except at energies very close to neutron thresholds. It is noted that the nuclear database of the electric giant dipole resonance (11) lacks sufficient accuracy in the energy region of astrophysical

importance as is evidenced by the non-vanishing values of the cross sections below threshold.

Figure 3 shows the experimental (γ,n) cross section on ^{181}Ta obtained with the LCS γ beam (34), compared with data recommended by IAEA on the basis of former measurements. Those data provided constraints on the low-energy tail of the dipole strength function. Their interpretation has necessitated a microscopic understanding of threshold behavior of photoneutron cross sections, showing the advantage of a QRPA calculation over a conventional Lorentzian- or hybrid-model analysis. The stellar photoneutron rate for ^{181}Ta was calculated in the Hauser-Feshbach statistical model with the QRPA result for the E1 strength. Those results have been used in (34) to re-examine the problem of ^{180}Ta in the p-process (see Sect. 6). Nuclear challenges remain in order to reliably evaluate the ^{180}Ta p-process yield. They include measurements of the ^{180}Ta photodestruction rate and the ^{181}Ta photo-neutron branching to the ^{180}Ta ground and first excited states (36). Such information would also help constraining reaction models.

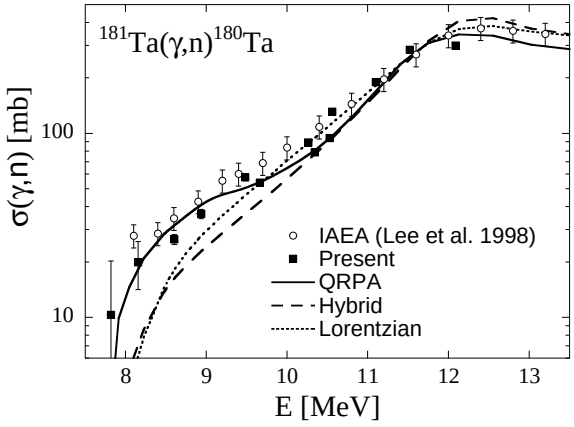

Fig. 3. Photodisintegration cross sections for ^{181}Ta(γ,n)^{180}Ta (34).

4.2 Data reduction

In nuclear astrophysics experiments, it is of crucial importance to provide absolute cross sections with high accuracy. Here we describe a methodology for deducing reliable cross sections from quasi–monochromatic photon-induced reactions.

The number of neutrons $n_{\rm exp}$ emitted in the photodisintegration experiment is related to the (γ,n) cross section $\sigma(E_\gamma)$ by its integral over the photon energy distribution $n_\gamma(E_\gamma)$:

$$n_{\rm exp} = N_{\rm T}\, h \int n_\gamma(E_\gamma)\, \sigma(E_\gamma)\, dE_\gamma, \tag{9}$$

where $N_{\rm T}$ is the number of target atoms per unit area, and h is the correction factor for a thick-target measurement, $h = (1-e^{-\mu t})/\mu t$ (with target thickness t and attenuation coefficient of target material μ). It is obvious that for ideally monochromatic photons with energy E_0, the integral is replaced by $N_\gamma \times \sigma(E_0)$ where N_γ is the number of incident photons.

Let us write $\sigma(E_\gamma)$ as a Taylor series,

$$\sigma(E_\gamma) = \sigma(E_0) + \sigma^{(1)}(E_0)(E_\gamma - E_0) + \frac{1}{2}\sigma^{(2)}(E_0)(E_\gamma - E_0)^2 + \cdots, \quad (10)$$

where $\sigma^{(i)} = d^i\sigma(E)/dE^i$. When the average energy is chosen for E_0, putting the Taylor series into the integral in Eq. 9 yields

$$\int n_\gamma(E_\gamma)\,\sigma(E_\gamma)\,dE_\gamma = N_\gamma\{\sigma(E_0) + s_2(E_0) + s_3(E_0) + \cdots\}, \quad (11)$$

where $s_2(E_0) = \frac{1}{2}\sigma^{(2)}(E_0)\,[\overline{E_\gamma^2} - E_0^2]$, $s_3(E_0) = \frac{1}{6}\sigma^{(3)}(E_0)[\overline{E_\gamma^3} - 3E_0\overline{E_\gamma^2} + 2E_0^3]$, etc., with $\overline{E_\gamma^i} = \int n_\gamma(E_\gamma)E_\gamma^i dE_\gamma/N_\gamma$. Note that $E_0 = \overline{E_\gamma}$, so that $s_1(E_0)$ vanishes.

Experimentally, from Eqs. 9 and 11, the bracketed Taylor series in Eq. 11 is deduced from the numbers of neutrons (n_{exp}) and incident photons (N_γ), as well as from the target properties. In order to obtain the cross section at the average γ energy, $\sigma(E_0)$, one has then to subtract the higher order terms s_2, s_3, etc.

Recently this procedure was exactly followed in the data reduction for the photodisintegration of ^{186}W (37). It was found that the subtraction resulted in only a few % increase in $\sigma(E_0)$ in the energy region of astrophysical relevance, where the energy dependence of the cross sections is dominated by the s-wave neutron emission ($\ell = 0$ in Eq. 3). Thus, the LCS γ ray is very close to monochromaticity at the energies of astrophysical interest.

5 The photoresponse of atomic nuclei below the neutron threshold

Because the thermal population of nuclear levels in stellar interiors has such a strong influence on the astrophysical photodisintegration rates, experimental studies on the photoresponse of nuclei below the particle threshold are of crucial importance for developing reliable models for such rates. In particular, a detailed knowledge about the structure of dipole excitations below the particle threshold is an important input for these models.

An ideal tool to investigate the photoresponse of nuclei below the particle threshold is real photon scattering or nuclear resonance fluorescence (NRF) (38). A "white" bremsstrahlung photon spectrum is produced by stopping an electron beam in a radiator target. This photon beam hits the target material and induces dipole and, to a lesser extent, quadrupole transitions to higher lying states. The γ decay of these states back to the ground and excited states is observed with high resolution ($\Delta E/E \simeq 0.1\%$) HPGe semiconductor detectors.

The pure electromagnetic excitation mechanism allows one to derive absolute transition strength or decay width of the excited states without any model dependency. Due to the high sensitivity of present set-ups one gets a rather complete picture of the dipole and quadrupole strength distribution in stable nuclei. Very recently the bremsstrahlung experiments have been complemented by $(\vec{\gamma}, \gamma')$ experiments using a polarized quasi–monochromatic photon beam from laser Compton backscattering (39). This method gives easy access to additional observables like parities and weak decay branchings.

The photoresponse of atomic nuclei is dominated by the giant dipole resonance (GDR). However, recent measurements have shown that a considerable part of the electric dipole strength remains in the $1\hbar\omega$ region i.e. around about 7 MeV in stable nuclei (40; 41; 42; 43) and is not shifted to the GDR. In heavier nuclei this strength seems to be concentrated in a resonance like distribution of 1^- states. This can be seen in Fig. 4 for the $N = 82$ isotones. The concentration of states between 6 and 8 MeV and the lack of strength at higher energies shows that these are not just statistical E1 excitations riding on the tail of the GDR but that the states have their own nuclear stucture. The summed E1 strength in this energy region exhausts up to one percent of the isovector energy weighted sum rule. A similar concentration of E1 strength has been found in lighter nuclei as well (44; 45; 46; 47).

In exotic nuclei with large neutron excess, up to 10% of the total isovector E1 strength has been found at very low energies, both in photodissociation and in Coulomb excitation experiments in inverse kinematics (48; 49). These experiments are a useful complement to the high precision (γ, γ') experiments on nuclei in the valley of stability.

The structure of the E1 excitations is still under intense discussion. Triggered by the experimental observation that nuclei with neutron separation energies of less than S_n=10 MeV possess a neutron skin, several models describe the mode as an oscillation of this skin versus the proton/neutron core (50; 51). In addition several microscopic calculations explain a considerable part of the E1 strength as a dominant isoscalar mode (43; 52; 53).

Upcoming experiments will extend the systematics of the E1 strength dis-

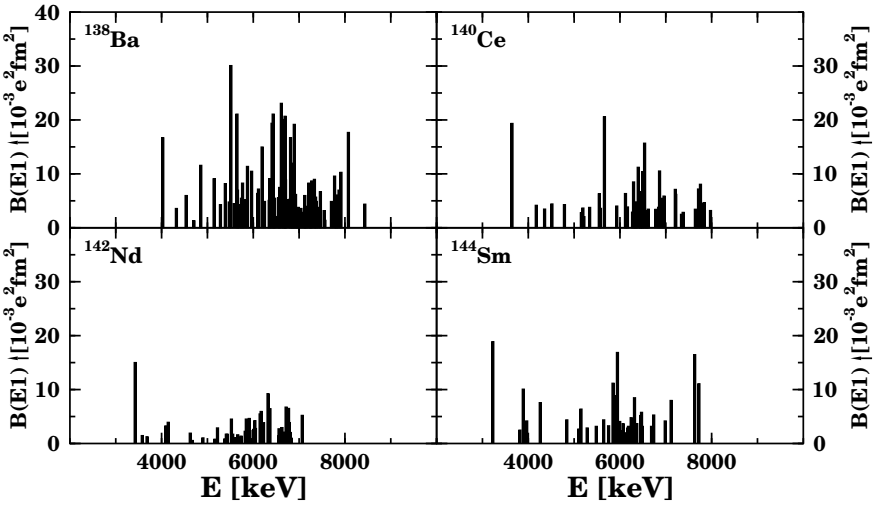

Fig. 4. Distribution of electric dipole strength in the $N = 82$ isotones ^{138}Ba, ^{140}Ce, ^{142}Nd, and ^{144}Sm.

tribution, will measure additional observables like the isospin character and detailed branching ratios and will look into the E1 response of exotic heavy nuclei. This will hopefully allow a deeper insight into the structure of the E1 modes around the particle threshold and finally allow more reliable model calculations of reaction rates with predictive power.

6 Astrophysical p-process

One question raised by the p-process studies is to know to what extend the calculated p-nuclei abundances do reproduce the solar system ones. A variety of explosive stellar sites in which matter is heated to temperatures in the range $T_9 = 1.5$–3.5 succeed in synthesizing p-nuclides with relative abundances in rough agreement with the solar system isotopic content. The only serious discrepancy concerns the large isotopic ratios of the Mo and Ru p-nuclei in the solar system (of the order of 10% of the corresponding elemental abundances), for which no satisfactory explanation has been found so far (see (4) for an updated discussion of this problem). The remaining less significant differences can be attributed to problems with the nuclear physics involved or with an inappropriate choice and/or a bad description of the stellar site(s) assumed to be at the origin of the solar system p-nuclei. Any reduction in the nuclear physics uncertainties will therefore put better constraints on the determination of the astrophysical sites to consider. As far as the global p-nuclei production is concerned and considering the very large number of nuclear reactions involved in the production of even a single p-nucleus, it is difficult to pinpoint one critical experimental information on which nuclear physicists should fo-

cus. Rather, any measurement of a photodisintegration cross section on nuclei which are located as close as possible to the p-process path and for energies in the appropriate Gamow windows should help gaining more confidence in the calculated rates, in particular in getting direct insight into the E1-strength function near particle threshold energies and in obtaining more reliable astrophysical photodisintegration rates without having to resort to detailed balance calculations.

Other problems raised by the p-process nucleosynthesis concern the production of the rare odd-odd nuclei ^{180}Ta^{m} and ^{138}La. In both cases (γ,n) reaction rates on these nuclei and on their much more abundant neighbors ^{181}Ta and ^{139}La are the essential nuclear quantities which will determine their final abundances.

The rarest stable nucleus in the solar system and the only naturally occurring isomer, ^{180}Ta^{m}, has been shown by (2) to be a natural product of the p-process in SNe-II. This conclusion was also largely shared by (3), with different stellar models and updated reaction rates. As seen in Sect. 4, the measurement of the ^{181}Ta(γ,n)^{180}Ta reaction cross section at energies close to the neutron threshold has provided a unique opportunity to improve the description of the E1-strength function and to obtain a more precise estimate of the astrophysical rate for that reaction. The problem of the ^{180}Ta production has been re-examined in (34) in the case of a 25 $M_{\odot}$ model star with solar metallicity, using the ^{181}Ta(γ,n)^{180}Ta rate constrained by the AIST experiment. The previous prediction that ^{180}Ta^{m} is produced at the same level as the bulk of p-nuclides in SNe-II has been quantitatively confirmed for a 25 $M_{\odot}$ SN-II and there are no reasons why different conclusions would be reached when the ^{180}Ta^{m} productions calculated for other stellar masses will be averaged over a stellar mass function, as done in (2). But on the other hand, the p-process origin of ^{180}Ta^{m} has to be confronted to the fact that this nuclide might (54) or might not (55) be produced by the s-process in AGB stars and that it is also expected to receive some contribution from ν_e-captures on pre-existing ^{180}Hf (56).

The rare odd-odd nucleus ^{138}La is generally underproduced in p-process calculations although it has been found recently that exploding sub-Chandrasekhar-mass CO white dwarfs could be significant ^{138}La producers (4). The problem of the ^{138}La underproduction in more conventional p-process sites like SNe-II has been addressed in (57). Two reactions are critical for the thermonuclear production of that nuclide, (1) ^{139}La(γ,n)^{138}La and (2) ^{138}La(γ,n)^{137}La. In order to produce ^{138}La at the mean level of p-nuclide production in the 25 $M_{\odot}$ model star considered in (57), the ratio of the rates for reaction (1) to reaction (2) had to be increased by a factor 20–25 with respect to the ratio obtained with HF (MOST) calculated rates. Such a large increase was very unlikely in view of an analysis of the nuclear physics uncertainties in the HF calculations. On the other hand (57) also re-examined the neutrino production of

^{138}La, originally proposed by (56), using an improved treatment of the (anti-)neutrino interactions, and confirmed that neutrino processes can compensate the thermonuclear underproduction of ^{138}La. However, if many of the input data necessary to calculate HF reaction rates have been measured for ^{139}La, in contrast, very little is known experimentally for ^{137}La or ^{138}La. Clearly the measurement of (γ,n) cross sections on ^{139}La and ^{138}La are very desirable to disentangle the weak interaction and thermonuclear origins of ^{138}La. Experimental values for the (γ,n) reaction on ^{139}La will soon be available from recent measurements at AIST. Similar measurements on ^{138}La are a very stimulating challenge for the future!

7 Perspectives

Synchrotron radiation facilities of the third generation are constructed in Europe (ESRF), America (APS) and Japan (SPring-8). They feature a variety of insertion devices as light sources. At SPring-8, a 10 Tesla super-conducting wiggler (SCW) was installed at the 8 GeV storage ring for a test production of a high-energy radiation.

As shown in Fig. 5, this radiation resulting from a 100 mA electron current is intense, even near neutron thresholds around 8 MeV (10^{7-8} photons sec^{-1} MeV^{-1} for a 10 T magnetic field) (58). More importantly, it is characterized by exponential tails which mimic the high energy part of Planck spectra corresponding to temperatures reached during the p-process. The SCW radiation can thus be used to directly determine the photonuclear reaction rate in Eq. 1 by activation techniques without such manipulation as the superposition of several bremsstrahlung spectra with different end-point energies (8).

Alternatively, the experimental parameters (σ_0 and ℓ) involved in the threshold behavior of the photoneutron cross section in Eq. 3 can be determined from a few measurements of the reaction rate with the SCW radiation at the highest available magnetic fields. Note that ℓ should be treated as an experimental parameter, because of a possible mixture of s- and p-wave neutron emissions.

There is a long list of photoreactions of interest for the p-process (not listed here) which can be studied with the SCW radiation at SPring-8. The photodisintegration of ^{180}Ta is certainly among them with a high priority.

The study of the photodisintegration of neutron deficient radioactive nuclei along the p-process path is also one important future project. Coulomb dissociation into the neutron channel where outgoing nucleus and neutron are measured in coincidence, is a promising experimental technique, the development of which is being considered at GSI.

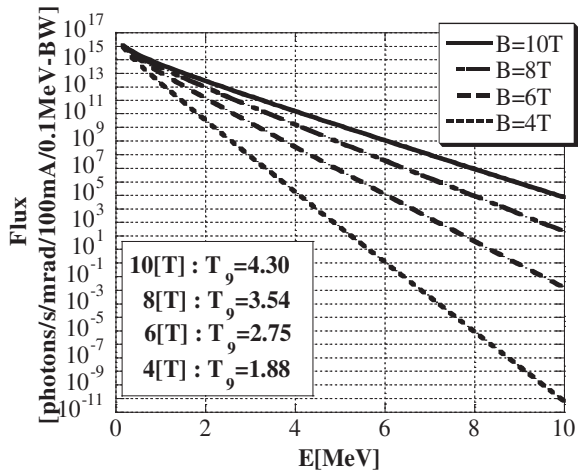

Fig. 5. Synchrotron radiation from a 10 Tesla super-conducting wiggler at SPring-8 (58). The temperature of the black-body radiation equivalent to the high-energy part of the SCW radiation is given for different magnetic fields.

The bremsstrahlung and the monochromatic LCS beam play complementary roles in the study of photon-induced reactions. With its intense photon source, the former technique allows photoactivation with natural target material because of the high sensitivity to radioactive species. A ground state photoreaction rate is determined with a superposition method which approximates the Planck distribution. The SCW radiation has the further advantage to be also able to determine the threshold behavior of (γ,n) cross sections. The latter photon source allows the cross section measurement over the Gamow window, which is the most direct way of testing the HF calculations of the rates. The direct neutron counting can be applied to any nuclei in principle, but in practice is limited to nuclei for which a considerable amount of enriched target material can be made available. It must be stressed however that there are presently certain regions in the valley of stability that are accessible neither by photoactivation nor by direct neutron counting, because some photoreactions result in the production of stable nuclei or of radioactive nuclei with extremely long half-lives, and because target preparation is made difficult for nuclei with very small natural abundances. Obviously, the emergence of a high-intensity monochromatic photon source is awaited with great interest.

8 Conclusions

Photon-induced reactions, (γ,x) (x= n, p, α, γ), have a direct impact on the nucleosynthesis of the p-nuclei. Among those, only (γ,n) reactions of direct interest for astrophysics have been investigated for selected nuclei, by photoactivation with bremsstrahlung and by direct neutron counting with the LCS γ-ray beam. The experimental data enhance the reliability and the pre-

dictive power of the Hauser-Feshbach model calculations of the astrophysical reaction rates. The measurement of (γ,n) reactions on many more nuclei will follow, but the investigation of (γ,α) and (γ,p) reactions in the energy range of interest is still a challenging prospect. In addition, the E1 and M1 γ strength functions below particle thresholds should be addressed in direct relation to photoreactions on nuclear excited states under stellar conditions. Photoreactions on unstable nuclei are however beyond the present scope except with the virtual photon source, Coulomb excitation/dissociation.

As demonstrated by the emergence of bremsstrahlung and laser inverse Compton γ rays, followed by the SCW synchrotron radiation, the development of lasers, accelerators and of related technologies will give fresh impetus to the creation of new γ-ray sources of great value for nuclear astrophysics.

Acknowledgements

We want to thank H. Yonehara, J. Enders, U. Kneissl, A. Richter, T. Rauscher, and S. Goriely for valuable discussions and private communications. The realization of the experiments at the S-DALINAC would not have been possible without the enthusiasm of the members of the photon group, especially M. Babilon, D. Galaviz, K. Sonnabend, K. Volz, and K. Vogt. The experiments at the AIST were made possible by the great efforts of H. Toyokawa, H. Ohgaki, K.Y. Hara, and S. Goko. This work was supported by the Japan Society of the Promotion of Science, the Japan Private School Promotion Foundation, and the DFG under contract SFB 634. M.R. is Research Associate of the National Fund for Scientific Research (Belgium).

References

[1] S.E. Woosley and W.M. Howard, Astrophys. J. Suppl. **36** (1978) 285.
[2] M. Rayet, M. Arnould, M. Hashimoto, N. Prantzos, and K. Nomoto, Astron. Astrophys. **298** (1995) 517.
[3] T. Rauscher, A. Heger, R.D. Hoffman, and S.E. Woosley, Astrophys. J. **576** (2002) 323.
[4] M. Arnould, S. Goriely, *Phys. Rep.* **384** (2003) 1.
[5] P. Mohr, M. Babilon, D. Galaviz, K. Sonnabend, K. Vogt, A. Zilges, *Nucl. Phys.* **A719** (2003) 90c.
[6] E.P. Wigner, Phys. Rev. **73** (1948) 1002.
[7] P. Mohr, K. Vogt, M. Babilon, J. Enders, T. Hartmann, C. Hutter, T. Rauscher, S. Volz, A. Zilges, *Phys. Lett. B* **488** (2000) 127.

[8] K. Vogt, P. Mohr, M. Babilon, J. Enders, T. Hartmann, C. Hutter, T. Rauscher, S. Volz, A. Zilges, *Phys. Rev. C* **63** (2001) 055802.
[9] P. Mohr, M. Babilon, J. Enders, T. Hartmann, C. Hutter, K. Vogt, S. Volz, A. Zilges, *Nucl. Phys.* **A688** (2001) 82c.
[10] M. Rayet, N. Prantzos, M. Arnould, *Atron. Astroph.* **227** (1990) 271.
[11] S.S. Dietrich, B.L. Berman, *At. Data Nucl. Data Tables* **38** (1988) 199.
[12] A.D. Antonov, N.P. Balabanov, Yu.P. Gangrskii, F.G. Kondev, S.G. Marinova, A.P. Tonchev, Kh.G. Khristov, V.D. Cholakov, Sov. J. Nucl. Phys. **53** (1991) 9.
[13] J.A. Holmes, S.E. Woosley, W.A. Fowler, B.A. Zimmerman, *At. Data Nucl. Data Tables* **18** (1976) 306.
[14] T. Rauscher and F.-K. Thielemann, At. Data Nucl. Data Tables **75** (2000) 1.
[15] P. Mohr, *Phys. Rev. C* **61** (2000) 045802.
[16] P. Demetriou, C. Grama, S. Goriely, *Nucl. Phys. A* **707** (2002) 142.
[17] S. Goriely, *Tours Symposium on Nuclear Physics V*, Tours, France, 2003, Eds. M. Arnould et al., AIP Conf. Proc. **704** (2004) 375.
[18] P. Mohr, J. Enders, T. Hartmann, H. Kaiser, D. Schiesser, S. Schmitt, S. Volz, F. Wissel, A. Zilges, *Nucl. Inst. Meth. Phys. Res. A* **423** (1999) 480.
[19] K. Vogt, P. Mohr, M. Babilon, W. Bayer, T. Hartmann, C. Hutter, T. Rauscher, K. Sonnabend, S. Volz, A. Zilges, *Nucl. Phys.* **A707** (2002) 241.
[20] S. Müller, Diploma thesis, Technische Universität Darmstadt, 2004.
[21] S. Goriely, in *Nuclei in the Cosmos*, eds. N. Prantzos and S. Harissopulos, Gif-sur-Yvette: Editions Frontières, 1998, p. 314.
[22] S. Goriely, private communication, 2004.
[23] T. Rauscher, private communication, 2004.
[24] T. Rauscher and F.-K. Thielemann, At. Data Nucl. Data Tables, to be published, (2004).
[25] E. Feenberg and H. Primakoff, Phys. Rev. **73** (1948) 449.
[26] R.H. Milburn, Phys. Rev. Lett. **10** (1963) 75.
[27] F.R. Arutyunian and V.A. Tumanian, Phys. Lett. **4** (1963) 176.
[28] L. Federici, G. Giordano, G. Matone, G. Pasquariello, P.G. Picozza, R. Caloi, L. Casano, M.P. de Pascale, M. Mattioli, E. Poldi, C. Schaerf, M. Vanni, P. Pelfer, D. Prosperi, S. Frullani, and B. Girolami, Nuovo Cimento **59 B** (1963) 247.
[29] V.N. Litvinenko, B. Burnham, M. Emamian, N. Hower, J.M.J. Madey, P. Morcombe, P.G. O'Shea, S.H. Park, R. Sachtschale, K.D. Straub, G. Swift, P. Wang, Y. Wu, R.S. Canon, C.R. Howell, N.R. Roberson, E.C. Schreiber, M. Spraker, W. Tornow, H.R. Weller, I.V. Pinayev, N.G. Gavrilov, M.G. Fedotov, G.N. Kulipanov, G.Y. Kurkin, S.F. Mikhailov, V.M. Popik, A.N. Skrinsky, N.A. Vinokurov, B.E. Norum, A. Lumpkin, and B. Yang, Phys. Rev. Lett. **78** (1997) 4569.
[30] A.M. Sandorfi, M.J. LeVine, C.E. Thorn, G. Giordano, G. Matone, and

C. Schaerf, IEEE Trans. Nucl. Sci. **NS-30** (1983) 3083.
[31] H. Ohgaki, S. Sugiyama, T. Yamazaki, T. Mikado, M. Chiwaki, K. Yamada, R. Suzuki, T. Noguchi, and T. Tomimasu, IEEE Trans. Nucl. Sci. **38** (1991) 386.
[32] H. Utsunomiya, Y. Yonezawa, H. Akimune, T. Yamagata, M. Ohta, M. Fujishiro, H. Toyokawa, and H. Ohgaki, Phys. Rev. **C63** (2001) 018801.
[33] K. Sumiyoshi, H. Utsunomiya, S. Goko, and T. Kajino, Nucl. Phys. **A709** (2002) 467.
[34] H. Utsunomiya, H. Akimune, S. Goko, M. Ohta, H. Ueda, T. Yamagata, K. Yamasaki, H. Ohgaki, H. Toyokawa, Y.-W. Lui, T. Hayakawa, T. Shizuma, E. Khan, and S. Goriely, Phys. Rev. **C67** (2003) 015807.
[35] K.Y. Hara, H. Utsunomiya, S. Goko, H. Akimune, T. Yamagata, M. Ohta, H. Toyokawa, K. Kudo, A. Uritani, Y. Shibata, Y.-W. Lui, and H. Ohgaki, Phys. Rev. **D68** (2003) 072001.
[36] H. Utsunomiya, M.S. Smith, and T. Kajino, *in Tours Symposium on Nuclear Physics IV*, eds. M. Arnould *et al.*, AIP Conf. Proc. **561** (New York: AIP), p.159.
[37] P. Mohr, T. Shizuma, H. Ueda, S. Goko, Y. Makinaga, K.Y. Hara, H. Hayakawa, Y.-W. Lui, H. Ohgaki, H. Utsunomiya, *Phys. Rev.* **69** (2004) 032801
[38] U. Kneissl, H. H. Pitz, and A. Zilges, *Prog. Part. Nucl. Phys.* **37** (1996) 349.
[39] N. Pietralla, Z. Berant, V.N. Litvinenko, S. Hartman, F.F. Mikhailov, I.V. Pinayev, G. Swift, M.W. Ahmed, J.H. Kelley, S.O. Nelson, R. Prior, K. Sabourov, A.P. Tonchev, and H.R. Weller, *Phys. Rev. Lett.* **88** (2002) 012502.
[40] K. Govaert, F. Bauwens, J. Bryssinck, D. De Frenne, L. Govor, and V. Yu Ponomarev, *Phys. Rev.* **C57** (1998) 2229.
[41] R.-D. Herzberg, C. Fransen, P. von Brentano, J. Eberth, J. Enders, A. Fitzler, L. Käubler, H. Kaiser, P. von Neumann–Cosel, N. Pietralla, V. Yu. Ponomarev, H. Prade, A. Richter, H. Schnare, R. Schwengner, S. Skoda, H. G. Thomas, H. Tiesler, D. Weisshaar, and I. Wiedenhöver, *Phys. Rev.* **C60** (1999) 051307.
[42] A. Zilges, S. Volz, M. Babilon, T. Hartmann, P. Mohr, and K. Vogt, *Phys. Lett.* **B542** (2002) 43.
[43] N. Ryezayeva, T. Hartmann, Y. Kalmykov, H. Lenske, P. von Neumann-Cosel, V. Yu. Ponomarev, A. Richter, A. Shevchenko, S. Volz, and J. Wambach, *Phys. Rev. Lett.* **89** (2002) 272501.
[44] U. Kneissl, K.H. Keister, H.O.Neidel, and A. Weller, *Nucl. Phys.* **A272** (1976) 125.
[45] F. Bauwens, J. Bryssinck, D. De Frenne, K. Govaert, L. Govor, M. Hagemann, J. Heyse, E. Jacobs, W. Mondelaers, and V. Yu. Ponomarev, *Phys. Rev.* **C62** (2000) 024302.
[46] T. Hartmann, J. Enders, P. Mohr, K. Vogt, S. Volz, and A. Zilges, *Phys. Rev.* **C65** (2002) 034301.

[47] M. Babilon, T. Hartmann, P. Mohr, K. Vogt, S. Volz, and A. Zilges, *Phys. Rev.* **C65** (2002) 037303.

[48] A. Leistenschneider, T. Aumann, K. Boretzky, D. Cortina, J. Cub, U. Datta Pramanik, W. Dostal, Th.W. Elze, H. Emling, H. Geissel, A. Grünschloss, M. Hellström, S. Ilievski, N. Iwasa, M. Kaspar, A. Kleinböhl, J.V. Kratz, R. Kulessa, Y. Leifels, E. Lubkiewicz, G. Münzenberg, P. Reiter, M. Reimund, C. Scheidenberger, C. Schlegel, H. Simon, J. Stroth, K. Sümmerer, E. Wajda, W. Walus, and S. Wan, *Phys. Rev. Lett.* **86** (2001) 5442.

[49] E. Tryggestad, T. Aumann, T. Baumann, D. Bazin, J. R. Beene, Y. Blumenfeld, M. Chartier, M. L. Halbert, P. Heckman, T. A. Lewis, J. F. Liang, D. C. Radford, D. Shapira, M. Thoennessen, and R. L. Varner, *Phys. Rev.* **C67** (2003) 064309.

[50] Y. Suzuki, K. Ikeda, and H. Sato, *Prog. Theor. Phys.* **C83** (1990) 180.

[51] J. Chambers, E. Zaremba, J.P. Adams, and B. Castel, *Phys. Rev.* **C50** (1994) R2671.

[52] D. Vretenar, N. Paar, P. Ring, and T. Niksic, *Phys. Rev.* **C65** (2002) 021301.

[53] G. Colò, N. Van Giai, P. F. Bortignon, and M. R. Quaglia, *Phys. Lett.* **B485** (2000) 362.

[54] R. Gallino, C. Arlandini, M. Busso, *Astrophys. J.* **497** (1998) 388.

[55] S. Goriely, N. Mowlavi, *Astron. Astrophys.* **362** (2000) 599.

[56] S.E. Woosley, D.H. Hartmann, R.D. Hoffman, W.C. Haxton, *Astrophys. J.* **356** (1990) 272.

[57] S. Goriely, M. Arnould, I. Borzov, M. Rayet, *Astron. Astroph.* **375** (2001) L35.

[58] H. Utsunomiya, K.Y. Hara, S. Goko, H. Akimune, T. Yamagata, M. Ohta, H. Ohgaki, H. Toyokawa, T. Hayakawa, T. Shizuma, P. Mohr, Y.-W. Lui, H. Ohkuma, H. Yonehara, K. Soutome, and M. Arnould, *Proc. The 8th Intern. Conf. Clustering Aspects of Nuclear Structure and Dynamics*, Nara, Japan, 2003, Nucl. Phys. A, in press.